Evaluation of C-C/SiC Pintle Anomalies in HT-6 Post-Test Photos

Randy Lee Marshall Space Flight Center March 2009

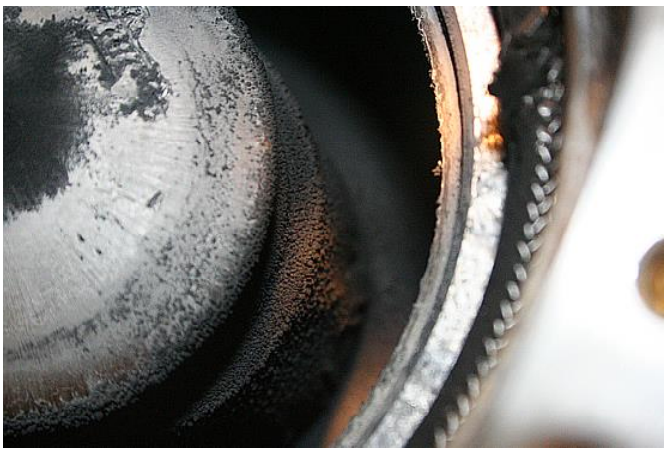

Observations:

(1) Regions are seen in which the outer surface layer has spalled away, exposing the under-surface, or under layer (the seal coat appears to have debonded from the under layer or substrate surface). (2) Microcracks can be seen across the pintle surface on both the outer layer and under layer surfaces. In some areas of the exposed under layer, a hexagonal-type pattern is apparent. (3) Small areas of cooled molten metal have been deposited on both outer and lower layer surfaces (indicating that the metal was deposited after the coating spalled). (4) Short gouge-like indentions or trenche-like features are occasionally seen within the under layer surface, protruding downward into the substrate below the under layer. The indention width is on the order of a fiber bundle diameter and is longitudinally oriented radially to the surface contour.

(5) Some of the spallations appear to have affected material below the level of the under layer, removing small sections of substrate matrix and/or fiber. The tire track effect is reflective of the *n*-D fibrous network comprising the structure of the substrate body. All images are looking down the *z*-axis (approximately)

Discussion:

Comments provided to these observations are given in generalized terms. While is not the intent to be vague, drawing conclusions or making far-reaching statements based on a few photographs would not be prudent. At this time, no physical measurements, EDX results, XRD, or any other form of data have been made readily available. It should be realized that at least some of the apparent damage seen in these photos occurred during the cool-down phase – after the burn cycle was complete, and some may have been present in the as-manufactured state. Images acquired during room temperature disassembly of the fired test valve can often be misleading, sometimes sending the analysts on wild goose chases trying to figure out how this or that particular anomaly is related to the apparent malfunction of the valve/motor. So the trick then becomes one of deciphering between manufacturing anomalies, cool-down effects and possible clues that might lead to better insight regarding the cause of failure during the actual burn cycle. However, there is no guarantee that this has necessarily been accomplished in the following essay. As such, it is felt that the best approach is started from a perspective that explores some of the relevant manufacturing steps that could be associated in some way or another with the observations seen in the photographs.

Each PIP densification cycle (Polymer Impregnation & Pyrolysis) consists of vacuum-augmented impregnation of the substrate using SMP-10 pre-ceramic polymer resin followed by pyrolysis of the resin-impregnated substrate to 1500°-1600°F which transforms the SMP-10 phase into glassy (amorphous) SiC ceramic, or a-SiC. Additionally, the substrate is subjected to 3000°F heat treatments after the 5th and 10th PIP cycles which then convert the glassy ceramic into the beta (cubic) polycrystalline form, β-SiC . . . as the transforming matrix recedes slightly and decreases in net volume. For the sake of clarity, once a-SiC is formed, the material does not soften or flow upon re-heating nor during thermal rearrangement into β-SiC. The effectiveness of only two high temperature treatments across 10+ PIP cycles is debatable. There is growing evidence that some of the pores, cavities and voids within the pre-coated substrate are not permeated during the standard XYZ/CC-SiC densification process, resulting in a finished product that apparently contains a significant level of impenetrable pore void volume, or 'closed' porosity.

After PIP cycle #10, machining of the slabs into the various section blanks and rough dimensioning is carried out (the last step prior to machining is 3000° heat treatment). After machining, many pores, voids and cavities are opened up and exposed to the outside. Thus, PIP cycles 11-13 are applied to the batch of freshly machined articles in single impregnation/pyrolysis runs (that is, the discrete parts are processed in batches rather than individually). These three PIP cycles are intended to fill up the exposed voids and opened pores created by the machining process, but it is also hoped that SMP-10 resin might permeate any residual porosity, tunnels and voids missed during the slab densification phase. There are indications however, that *the porosity network within the FMI/CC-SiC substrate does not appear to be interconnected*. It is suspected that a certain fraction of the pores, voids and cavities are permanently sealed off during the first few densification cycles. These volumes then become increasingly isolated and shielded as subsequent densification layers are packed on. One of the primary reasons for subjecting the substrate to intermediate high temperature treatments is to open up these passageways prior to the next impregnation cycle.

It is worth noting that the highest process temperature the articles see after the 3000° treatment following PIP cycle #10 is 2200°F. While pyrolysis temperatures during PIP cycles 11 thru 15 and Seal Coats 1 thru 4 each reach the 1550° range, only a single 2200° heat treatment is applied during the latter stage of the process (specifically, in between Seal Coats #2 and 3). After the 2200°F step, two more layers of Seal Coat slurry (#3 and 4) are brushed on with 1550° pyrolysis treatments in between and then the articles are subjected to two final 1550° PIP cycles (Seal Coat brush-on slurry consists of SMP-10 resin + leveling agent + SiC particles). Interestingly, these last two PIP cycles are

applied to articles which have already been seal coated. They are likely intended to force polymer into any residual surface porosity, to permeate any newly opened pore channels which might have interconnections into the substrate, and to level out the overall finish across the articles. One could say that PIP cycles # 11-15 actually form part of the coating phase or outer layers. The weight gains achieved from PIP cycles 14-15 are probably quite low. It is worth noting that each PIP cycle and Seal Coat application leave a remnant layer of glassy SiC on the surface of the articles. Also, all the process temperatures applied after machining essentially ensure a condition in which the majority of the peripheral SiC phase and surface coating contributions remain in the amorphous a-SiC state. It is presumed that this is the expected intention, given the potential properties that could be achieved with this approach. (Many aspire that a gradual transition between the glassy phase and the crystalline phase is established (a microstructural gradient transition zone), forming a powerful bond between the two structures, but this is debatable and unfounded).

The accompanying figure (inferred from XYZ's indicated manufacturing flow) should help illustrate the various processing layers that generally exist on finished articles. However, caution is exercised since the *time-temperature profiles* utilized by XYZ during processing of each layer are unknown (these are usually company proprietary). Ideally, knowledge of the individual time-temperature profiles would be supplemented by also considering the cumulative effects of subsequent treatments on the under layers as each layer is sequentially applied and processed.

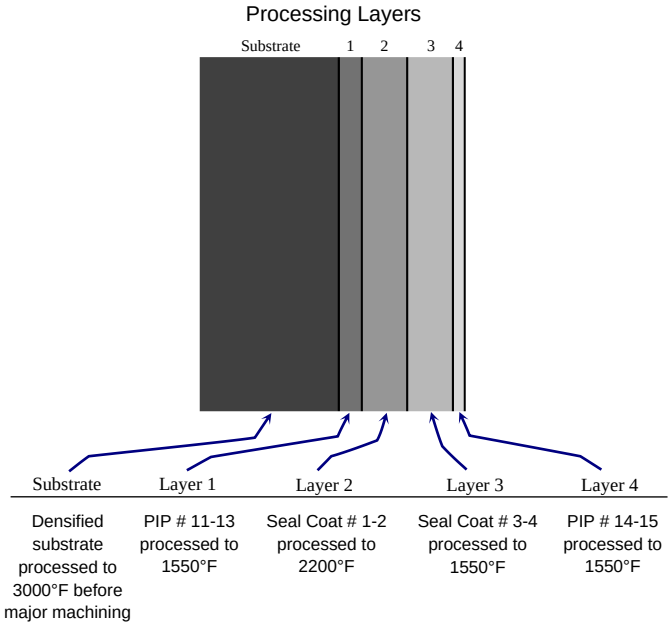

Thus, each PIP cycle and Seal Coat application deposits a layer of converted SMP-10 on the surface of the articles . . . but all the layers are not necessarily formulated or processed the same. Layer-to-layer differentials are expected in terms of layer thickness, degree of ceramicization, nature of adhesion to the adjacent layers and formulation make-up. Presumably, all articles undergo the same 1550F° rapid inert pyrolysis process (that is, there are no differences in the pyrolysis conditions, hardware, gas flow or gas composition). Thus, the primary difference between layers deposited via PIP impregnation and brush coating must be dependent on the specific properties achieved from each approach.

Vacuum-augmented PIP layers will be thinner and more uniform in thickness. They will also be less porous and more consolidated than Seal Coat layers which are loosely brushed (or painted) on. Brush-on Seal Coat slurries containing SiC particles exhibit much higher and irregular thicknesses. They will also be higher in porosity and lower in bulk density than vacuum impregnated PIP layers. While PIP impregnations saturate the inner porosity of the substrate, they also leave an outer coating on the surface of the article that is very tightly bound. PIP layers conform more precisely to the shape and contour of the substrate or under layer while brush-on layers exhibit more of a filling effect with the tendency to hide contour variations and surface irregularities. A more in-depth description of the causes behind these layer-to-layer variations is in order, and the emphasis will be placed on how well the interfaces are bonded to each other, before, during and after the burn cycle. This is best approached by considering some of the property differences between the layer phases as well as the chemical and mechanical bonding mechanisms at work along each of the interfaces.

If held at temperature long enough, the a-SiC phase will begin to undergo crystallation as low as 2000°-2200F°. Similarly, if held for at least several minutes at temperatures > 2600°, fine particles of crystalline SiC will begin to undergo solid state sintering via surface diffusion. Rapid exposure to 3000°+ can possibly reduce the initiation period for these reactions down to seconds. Long duration 3000F° heat treatments applied during the primary C-C/SiC densification steps imply that the inner matrix fraction is comprised almost exclusively of highly crystalline β-SiC . . . with all the properties of such, including conductivity, CTE, density, etc..., while layers forming the outer regions of the article consist heavily of glassy a-SiC, whose properties differ markedly from those of β-SiC (including conductivity, CTE and density). Even though both polymorphs are stoichiometrically identical, *the properties of a-SiC are not equivalent to those of β-SiC* (nor do they reflect the properties of hexagonal α-SiC which begins to form above the 3100°-3300F° range). Glassy (vitreous,amorphous) a-SiC is a unique form of SiC which has been recognized only recently, primarily as a result of the pre-ceramic polymer industry from which it is characteristically derived. As expected, crystalline structures conduct heat, mechanical and thermal shock waves more readily than amorphous structures. The fact that the conductivity, CTE and density of a-SiC are all substantially lower than that of β-SiC has been confirmed and well documented by Starfire scientists, personal testing experiences and a host of industry workers during the last two decades (some of these values will be evaluated later).

For the time being though, the ceramic portion of the matrix within the C-C/SiC substrate can be taken as ~100% β-SiC, while all the outer layers consist overwhelmingly of a-SiC. Due to the 2200° treatment after Seal Coat #2, Layers 1 and 2 may contain a small fraction of beta character, with most of that concentrated toward the outside of Layer 2 and gradually diminishing inward. Undoubtedly, there is a microstructural differential between the β-SiC matrix in the substrate and the a-SiC comprising most of Layer 1. However, despite the process temperature differential separating the 3000° substrate from the 1550° Layer 1 phase, other factors incorporated by the process are believed to drastically enhance bonding interactions between the substrate and Layer 1. Similarly but in contrast, while process temperatures for Layer 1 and Layer 2 not too different, other process factors are believed to significantly weaken the interface separating Layers 1 and 2. These factors are covered in the next section. For now, it can be pointed that the final 2200° treatment at the end of Layer 2 processing probably facilitates the cohesive properties *within* that layer more than it enhances bonding actions along the Layer 1 interface.

If post-machining process temperatures were high enough to promote sintering of the SiC particles (in Seal Coat layers 1-4), the intrinsic strength and cohesive energy would increase and the two Seal Coat layers might even fuse together. However, none of the thermal processes applied during these layering processes are high enough to initiate particle sintering, so they simply remain embedded within the coating layers as inert fillers (possible sintering effects are dealt with in the section, 'Burn Cycle – Cool Down Analysis'). Also, there is no historical evidence supporting the notion that the SiC microstructure comprising either one of these phases breaks down during customary processing practices or that elemental Si or C participate in any form of surface diffusion with adjacent interfaces. While these effects can be innovated into systems such as this in order to develop extraordinarily strong bonding phases and fused bimaterial interfaces, they appear to have little relevance to the current CMC platform under study. Furthermore, it seems that chemical binding effects between a-SiC and β-SiC phases may be not be as significant as expected (chemical bonding concepts and functional gradient transition zones are considered in a short discussion at the end of the report). Often, the approach has focused too heavily on the temperatures applied during processing and the resulting CTE incompatibilities, but process temperatures alone simply cannot tell the entire story regarding the nature and strength of these interfaces.

The degree or balance of chemical bonding and mechanical interlocking between layer interfaces is not only influenced by process temperatures, but is also heavily dependent on the particular process application used to deposit each layer.

During a typical PIP impregnation step, the articles are suspended or fixtured inside the chamber and the lid is vacuum-sealed and tightened down. The chamber is evacuated under medium vacuum for 30-60 minutes and resin is slowly drawn into the chamber (using the force of vacuum) until the articles are completely submerged in resin. Keep in mind that under vacuum, a liquid's boiling point is lowered accordingly and at some point during the intrusion process, the resin begins to boil (thus, these resins tend to foam and splatter inside the chamber, sometimes violently). The chamber is then slowly vented to equilibrium with the atmosphere (nitrogen is sometimes used as the filling gas since SMP-10 resin is susceptible to hydrolysis and oxidation). Venting and removal of the articles from the chamber stabilizes the intrusion at 14.7 psi atmospheric. The articles are lifted out and suspended above the opened chamber momentarily as excess surface resin drains back into the tank and is used for future impregnations. This often results in a self-leveling effect and a sort of 'glaze' of gelled resin across the surfaces of the articles. Sometimes, the operator may lightly blot some of the excess resin from the articles using a paper towel.

Since there are no condensation reactions involved during cross-linking of SMP-10 polymer or mass out-flux of solvents and volatiles released during ceramicization (other than hydrogen), the impregnated articles can be directly fired (pyrolyzed) from the wet state. However, personal innovations in this area have confirmed the fact that the application of pressure after venting (as part of the impregnation process), followed by curing of the impregnated articles *under pressure* substantially improves the degree of porosity intrusion and the ceramic yield markedly. This single aspect is crucial enough to note certain historical cases where CMC articles containing high levels of closed porosity associated with 'vacuum only' densification procedures underwent catastrophic failures during their maiden test cycles. It is unknown if XYZ utilizes pressure in any of their processes . . . since many CMC manufacturers do not, it is suspected that XYZ does not either. It is considered to be inconvenient, requires an upgrade from vacuum chambers to pressure vessels and possibly imposes a greater safety concern during processing. A lot of companies just don't like to use pressure, despite the evidence clearly demonstrating its benefits.

In any case, with this method, the powerful vacuum forces facilitate displacement of the air inside the pore network as resin intrudes deep into the accessible voids, pore tunnels and cavities. This approach overcomes the opposing capillary forces and surface tension effects which hinder the effectiveness of other methods (namely, passive application techniques such as dipping or brushing). Also, studies and experiments have demonstrated that impregnations performed in this manner are equally effective over a wide range of resin viscosities (surprisingly, thick and thin fluids yield about the same weight gain). However, the effects of gravity can negatively influence the distribution of resin within the article when it remains in one place for extended periods of time.

Nevertheless, when applied to freshly machined articles containing high levels of surface porosity (with interconnections into the inner substrate), vacuum-augmented ceramic resin intrusion forms an expansive network of dendritic fingers which extend deep into the substrate. These mechanical interlocks are quite significant and they physically/mechanically join the deposited surface layer to the inner substrate in a very unique manner. Thus, PIP cycle #11 permeates deep into the exposed pores of the machined articles and after pyrolysis, very strong, far-reaching mechanical bonds or interlocks are established. Indeed, the ceramicized surface layer deposited from cycle #11 is mechanically bonded to the substrate unlike any of the subsequent layers could ever expect to

achieve. In the process, most of the exposed substrate voids are filled with freshly deposited a-SiC from PIP cycle #11, and then the surface porosity diminishes rapidly as PIP sub-layers #12 and 13 are applied. Thus, Seal Coating #1 has little porosity to grab into.

Seal Coat layers are applied simply by brushing (painting) the slurry onto the articles by hand at ambient (room) conditions. The method is highly dependent on user technique so it is subject to skill variation and human error. No vacuum, pressure or temperature is applied except the standard 1550° pyrolysis performed after each brush application. To be inclusive, the XYZ C-C/SiC slurry formulation consists of liquid SMP-10 resin, fine crystalline SiC particles (β-, α- or a mixture thereof), a proprietary surfactant which enhances surface leveling and wetting effects and . . . entrenched air (air is automatically incorporated into particulate slurry suspensions during mixing, preparation and application). Entrenched air is known to be present in these types of systems to levels as high as 25-30%. Thus, compared to other deposition techniques, brush-on layers generally go down thick and bulky and at highly irregular thickness levels. During low temperature, pressureless firing, consolidation is minimal and afterwards, these layers may contain substantial levels of porosity, both open and closed. Firing also destroys the organic surfactant layer which chars and volatilizes above 550°-600F°, leaving small occlusions and discontinuities along the particle interfaces.

More importantly, the particles in these types of slurries tend to agglomerate (due to electrostatic surface charges) unless specialized dispersing agents are incorporated into the formulation mix (the leveling agent used in the current Seal Coat slurry is not a ceramic particle dispersant). It is also known that particle agglomerates will collect at pore entrances preventing the flow of intrusion fluid into the pores of the substrate. The use of particulate slurries during CMC substrate densification procedures was practiced for a while until the industry realized the detrimental effects they produced (namely, large fractions of closed porosity and trapped gases) which was often followed by delaminations and catastrophic failures during thermal testing. The use of vacuum and/or pressure during these types of processes is of little help since the hard particles often wedge into pore tunnels and cavities permanently constricting the passageways. In any case, during the FMI process, there are absolutely no intrusion/impregnation/infiltration techniques applied to try and force the slurry into the pore network of the under layer. The brushing action is ineffective in this regard since capillary forces will limit displacement of the pore gases and tend to restrain the resin at the pore openings. With the current Seal Coat brush-on technique, there is little surface penetration and thus, few mechanical interlocks are ever established after application and firing.

Considering the smooth, essentially non-porous condition characterizing the surface of PIP sub-layer #13, mechanical interlocking with Seal Coat #1 is not expected to be very significant. Additionally, the process temperatures are too low to facilitate any notable level of chemical or ceramic bonding between Layers 1 and 2. Bonding interactions between Layers 2 and 3 are enhanced due to the porosity of Layer 2 and the similarities in application method, while strong adhesion effects are also expected between Layers 3 and 4 due to mechanical interlocking of PIP sub-layer #14 to the porous Seal Coat layers. Thus, from a purely mechanical perspective, the interface separating Layers 1 and 2 is expected to be the weakest and most vulnerable interface in the entire system, while the interface joining Layer1 to the substrate is ladened with penetrating mechanical interlocks. This is reflective of the physical/processing differences and the ultimate results achieved between layers deposited via forced intrusion of straight resin directly into the substrate pores vs. ambient passive overlay of thick particulate slurries onto smooth, low porosity surfaces.

Sources for Variation

Unfortunately, variations in the properties of the layers and their interfaces are ever-present and often lead to regional areas or localized ‘patches’ of weakened material which seem to behave

differently than the surrounding material. These effects are hard to predict and sometimes appear to occur randomly but they are suspected to have strong dependencies on variations in the machining process, the specific contours and geometries of the article, brush application techniques (from one article and operator to the next), and/or the specific configuration of the articles within the impregnation chamber, the pyrolysis furnace or the retort, or a combination of any of these. Examples of possible defects associated with configuration variations could include (a) articles in direct contact with each other during impregnation or with the impregnation chamber wall or the retort wall or any supporting structures inside these containers (prior to both impregnation and pyrolysis, the batch of articles must be properly suspended, oriented and restrained in the reaction chamber with the appropriate hardware), (b) inadequate distribution of liquid resin due to localized hydraulic constrictions or gravity effects, entrenched air pockets or foaming of the resin, FOD contamination, movement of the parts during the impregnation process (the instant the resin enters the vacuum chamber, it is suddenly forced to occupy the chamber volume and this can sometimes agitate the contents), abnormal viscosity variations or localized over-staging (including over-staged, localized globule regions indicative of pre-mature cross-linking or out-gassing of the resin), and (c) inadequate gas flow and heat distribution during pyrolysis.

Other factors with an appreciable probability of contributing to variations within the material include (a) localized pore clusters and abnormal regional porosity within the substrate (this will be considered in greater detail later), (b) variations in polymer composition; for instance, inadvertent regional concentrations or depletions of allene (cross-linking) side groups or siloxane linkages resulting in abnormal localized expulsions of hydrogen, silicon oxides and/or aliphatic hydrocarbons, and (c) localized regions of abnormal pyrochemistry resulting in silicon-rich or carbon-rich domains, both of which can adversely affect binding characteristics with adjacent interfaces (possibly resulting in reaction-bonding effects in lieu of true SiC-to-SiC bonds). These last two factors are based on specific characteristics associated with the synthesis and thermal conversion SMP-10 resin. While hydrogen is overwhelmingly the primary reaction gas generated as SMP-10 cures and pyrolyzes, lesser amounts of methane, ethane and ethylene are also emitted during these processes (even smaller amounts of SiO_2 and water are also known by-products). Along with the use of nitrogen during SMP-10 storage and densification processing at XYZ, these are also the gases expected to occupy most of the trapped voids and closed porosity within the substrate.

Contributions to the fraction of closed porosity in these systems are known to be influenced by (a) resin blockage during impregnation which can be affected by capillary forces or any of the factors discussed earlier, (b) inadequate pore network interconnectivity, which could also be influenced by these other factors but is especially dependent on the frequency of 3000F° treatments applied throughout the densification process, (c) less-than-effective impregnation procedures; ideally, freshly impregnated articles should be pressurized while still in the chamber (after venting) and most importantly, they should be cured under pressure to ensure that the resin remains in the pores.

Burn Cycle – Cool Down Analysis

Physical property differentials across the interfaces can be significant, and after a test fire, it can sometimes be difficult to visually ascertain which anomaly happened during the burn cycle, during cool down, or was previously incorporated somewhere in the manufacturing process. For the moment, it might be interesting to consider how each of the constituents respond to the forces of thermal expansion and contraction.

The confirmed CTE range of SMP-10-ceramicized polycrystalline β-SiC runs around 4.0-4.5 (ppm/°C), while that of its glassy counterpart a-SiC, is now known to be about 2.3-2.5 (a potential mismatch factor of 2 is possible between these two SiC forms). Additionally, the densities of the two

phases are known to be about 2.9-3.1 (g/cc) and 2.4-2.6 respectively (depending on the method of application and consolidation). Thus, both α and β-SiC > a-SiC, and for all practical purposes, both β-SiC and a-SiC are recognized as isotropic phases. On the other hand, the carbonized PAN fibrous reinforcement constituent in the substrate is highly orthotropic with a longitudinal CTE that is almost nil and a lateral or transverse CTE that is known to run somewhere in the 4-6 range (that is, the fibers get fatter while their lengths remain about the same). Thus, along directions parallel to the fiber bundle diameter, expansion/contraction effects of the reinforcement and SiC phase are comparable and compatible, but along longitudinal fiber directions, the β-SiC phase tends to expand and contract ~ 4 times greater than the fiber surface, so these interfaces are subjected to significant stresses during heat-up and cool-down events. As a matter of fact, longitudinal fiber-to-matrix interfaces represent the primary CTE mismatch within the C-C/SiC system. Thus, during thermal excursions, the following remarks can be made (reference the process layer diagram given earlier).

In the substrate phase, the fibrous reinforcement tries to constrain the expanding matrix, or conversely, the matrix tries to pulls the fiber bundle along with it, so the effective (overall, net or resultant) CTE of the substrate is somewhere in between 0 and ~4, perhaps close to midway, give or take, depending on the relative strengths and moduli of the constituents, as well as the precise orientation of interest. Now the mismatch directly along the fiber interfaces is still ~4, which creates Mode II shear forces along these interfaces subjecting the fiber surfaces to tension and the matrix to compression as the entire composite body thermally expands. During contraction however, the stress situation reverses, placing the fiber surfaces under compression and the matrix under tension. Microcracks will tend to form in materials when they are placed under tensional forces. Even though the compressional strength and modulus of the fiber are almost insignificant, there is still a slight chance that some matrix microcracks could initiate during the cool-down stage.

Along the interface separating the 3000F° substrate and the 1550° Layer 1, longitudinal fiber bundle surfaces directly interfacing the a-SiC of Layer 1 (or more precisely, longitudinal vector components of the fiber bundles contacting the interface at various angles) become weak points with a range of mismatch factors topping as high as ~2. Also, β-SiC-to-a-SiC domains in contact along the interface may exhibit mismatch factors as high as ~2. So the substrate longitudinally expands and contracts almost twice as much as Layer 1 . . . not as high as the quadruple mismatch along the fiber surfaces in the substrate but high enough to place Layer 1 under tension during the burn cycle when it is believed that microcracks form in this layer. (As long as Layers 2, 3 and/or 4 remain intact at temperature, the substrate is protected). During cool-down, the stress condition reverses and the cracks in Layer 1 will tend to close up, but concurrent processes taking place in Layer 2 could affect these closure gaps. Due to direct interfacial contact with the substrate, the pattern projected through Layer 1 by the microcracks will tend to reflect the hexagonal structure of the n-D reinforcement underneath since the outer-most fiber bundles along the substrate interface become the primary stress concentration points (or ridges) when the system is heated up and cooled down.

Due to the 2200° treatment applied after Seal Coat #2, Layer 2 may contain low levels of beta character but Layers 3 and 4 are composed exclusively of glassy a-SiC . . . until the test cycle begins. Upon ignition, the burn cycle rapidly reaches the 3000°+ range. At some point, the outer layers begin to undergo thermal crystallization, Layer 4 first, then Layer 3 and possibly some of Layer 2. The conversion process (from a-SiC to β-SiC) results in moderate volumetric shrinkage of the affected layers, producing cracks, and possible recession effects or 'islands'. As the outer layers crystallize, a thermal mismatch with Layer 1 develops subjecting the Layer 1-to-Layer 2 interface to Mode II shear forces as Layer 1 is placed under tension while Layer 2 is diametrically placed under compression. As the system cools down, the stress situation reverses placing the outer layers under tension where microcracks are believed to form during cooling. Before the burn cycle ends however, particle sintering in Layer 3 and possibly 2 may eventually start to take place, tending to strengthen these

layers and enhancing the possibility of interface fusion. Layer 4 is mechanically bonded to Layer 3 fairly well but considering the thinness of Layer 4, along with the apparent brush marks on the outer surfaces in the photos, regions of Layer 4 may have burnt off during the test cycle. Also note that reaction products from oxidation of the solid propellant upstream may facilitate the formation of a thin layer of amorphous silica across sections of the SiC surfaces, possibly leading to the temporary appearance of a 5th layer during the early stages of the burn cycle.

The CTE mismatch between the substrate and Layer 1 is moderately significant. However, due to the freshly machined substrate surface, Layer 1 mechanical interlocks are so pervasive that the effects of the CTE differentials are subdued and Layer 1 is considered to remain strongly attached to the substrate during the burn cycle and the cool-down phase (as long as no other weakening factors are prevalent such as excessive closed porosity near the substrate periphery which can negate the mechanical interlocking effects). The CTE mismatch between the a-SiC-dominated Layer 1 and β-SiC rich Layer 2 may be as high as ~1.5-2 while the degree of mechanical interlocking connecting these two layers is insignificant. Thus, *the interface separating Layers 1 and 2 is the weakest interface in the system and appears to be the level where most of the spallations occur . . . during the burn cycle*. The particular areas or patches where spallations happen to occur are probably associated with material variations, some of which were alluded to earlier. Before the burn cycle ends, under layers which have been exposed due to spallation are susceptible to thermal crystallation.

If clusters of closed pores and/or large voids are present in the substrate just below Layer 1, a spallation event could become more extensive, possibly excavating sections of the substrate matrix in the process. Alternatively, if by chance some kind of debris grazed the surface of the pintle during the test cycle very close to a weakened porous area below, it is possible the impact damage could facilitate excavation, possibly extracting a small section of the material, and revealing the inner substrate structure underneath. In any case, clustered pores of this nature are uniquely prevalent in this particular C-C/SiC system and spallation/excavation of material could conceivably produce the apparent 'tire track' effect seen in one of the photos (this type of porosity is addressed below).

The Nature of Porosity

Apparent variations in the distribution, dimensional characteristics and inter-connectivity of porosity in the C-C/SiC system are a matter of concern. One of the photos taken after disassembly of the tested HT-6 valve gives a cross-sectional view of the assembly, visually revealing the inner structure of the C-C/SiC material.

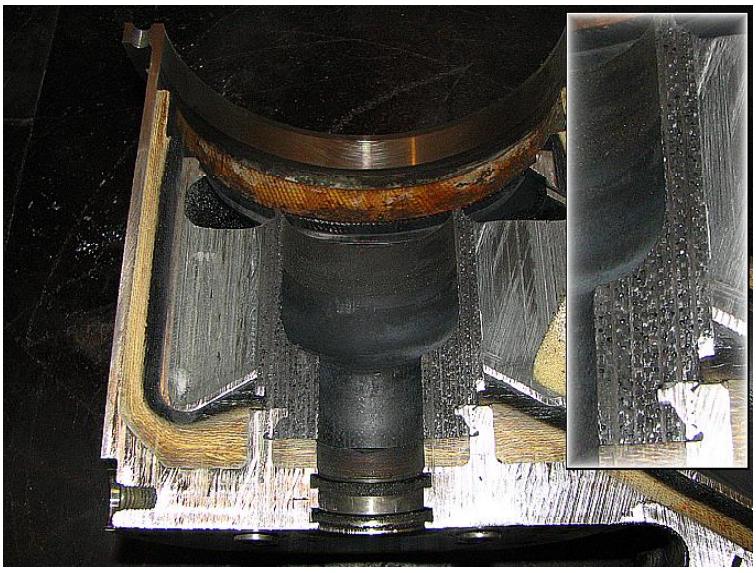

The accompanying photo is probably representative of the average macro-porosity that exists below the surface layers in all these articles. Without a doubt, many of these voids were sealed off sometime during the substrate densification process, perhaps during the first few cycles. The image also reveals a few regions where voids are spaced very close together and they almost appear to be combined in some spots. Pore clustering, oversized cavities and excessive regional porosity are obviously undesirable and are believed to be responsible for some of the anomalies seen in the HT series of

post-fired pintle articles examined recently. For the XYZ C-C/SiC system, a symmetrically spaced network of voids is apparent and is directly related to the particular weaving architecture of the preform. It has already been documented in previous studies that these voids, cavities and clusters are most prominent at the *u-v-w-z* fiber bundle intersections. Smaller porosity volumes seem to occur more randomly throughout the matrix and constituent interfaces. It is obvious that SMP-10 resin is not penetrating many of these intersection voids and there are no indications that the network of intersection voids is interconnected to any regular degree. The particular locations where these voids form can be visualized by considering the specific structure of the n-D preform. The accompanying illustrations give an example of the void pockets which are possible in locality to the fiber bundle intersections from the three primary axial perspectives.

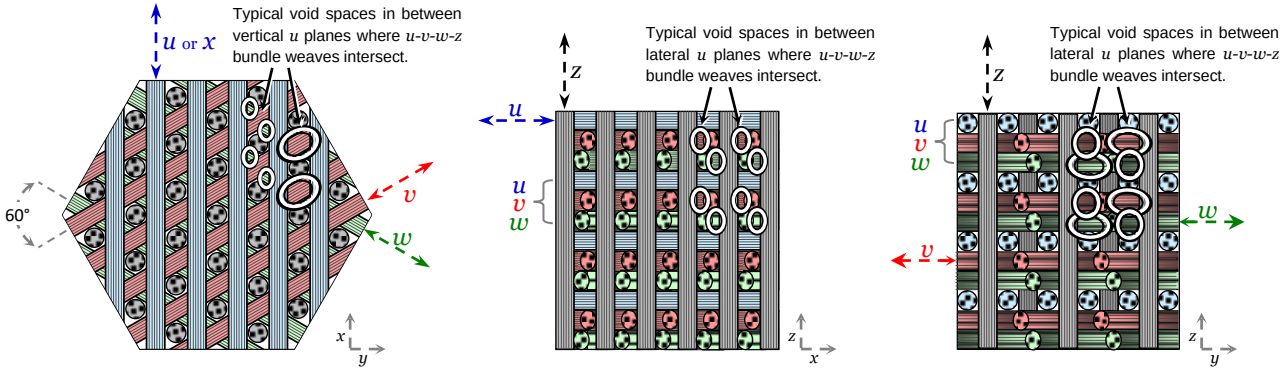

In general, each view gives a different perspective of the same voids but some cannot be seen well in all views so all three perspectives are necessary to grasp the full extent of these intersection voids. Circled spots are only representative examples of the spaces that symmetrically exist *at all* the bundle intersections across each plane of bundles. Most of the voids in the composite are occupied to varying degrees by the matrix resin. But the evidence has already shown that a substantial fraction of the intersection voids have not been appreciably densified, sometimes forming arrays, rows, columns, groups or clusters of unoccupied or closed voids. Voids of this type occurring occasionally on one side of a given *u-v-w-z* intersection (or even a periodic array along one of the *u-v-w-z* planes) would not necessarily be considered detrimental.

However, the greatest concern arises when adjacent corners within the locality of a given *u-v-w-z* intersection are also void, as well as adjacent voids within the same intersection. In these cases, *local clusters* of voids are created and they are so close to one another that the immediate region is undoubtedly in a weakened state . . . adjacent voids within the intersection may be in direct contact, nearly in-contact or merged together creating large cavities and potential excavation sites. Clearly, localized regions populated with these kinds of closed void clusters *are not* going to reflect the same mechanical properties as other regions containing less porosity or uniformly dispersed voids. While it may appear as though sections of matrix were removed in some images, in actuality, some or all of the closed cavities in a local cluster were simply exposed during the excavation process. Or perhaps machining damage weakened some of the peripheral fiber-to-matrix interfaces resulting in a combination of matrix excavation and void exposure producing the tire track effect (the consequences of machining damage are treated in the next section).

Recall the statement earlier concerning the primary expansion/contraction mismatch in the substrate along the longitudinal fiber-to-matrix interfaces. Well, from a contrasting viewpoint, the stress condition is actually subdued as a result of the porosity along these interfaces. Despite the obvious mechanical degradative effects, stress relief is one of the benefits of residual porosity in these

types of composites, along with improvements in shock resistance and toughness. Nevertheless, the negative effects of *excessive* localized porosity and large void clusters far outweighs the benefits of any stress relief they might provide. Unfortunately, excessive porosity will have detrimental effects that can often lead to catastrophe. Controlled levels of uniformly distributed porosity fractions are desirable but localized clusters and extra large cavities have been repeatedly indicated as a principal source for weakness in composite materials and are often directly associated with the root cause of significant failures. The presence of large voids and localized pore clusters of this type should be considered carefully because they are not the desired product of the C-C/CMC engineer.

Ideally, a uniformly distributed interconnected porosity structure is preferred – with a balance of micro-, meso-and macro-porosity to effectively facilitate simultaneous resin intrusion and volatile removal (macroporosity generally comprises the majority of a composite's volumetric porosity fraction). In this situation, the resin impregnates or intrudes into the substrate by progressing through the macropores (holes, voids, tunnels, cavities and cracks that are > 50nm in diameter or their smallest dimension of passage), while all the escaping volatiles pass out of the system through the mesopores (2nm < d < 50nm) and micropores (< 2nm). In the previous photo as well as any similar photo, only (some of) the macroporosity can be seen with the naked eye or under low magnification. Meso-and micropores can only be revealed under SEM or extremely high optical magnification methods. Undoubtedly, XYZ measurements of porosity in the ~13% range are not inclusive. They only approximate the 'open' porosity which is available to the particular intrusion fluid and technique used to make the measurements. Much of the closed porosity, meso- and micropores are not susceptible to Archimedes-type porosity testing, and so the total porosity in this material is probably a lot higher than the reported values, perhaps double.

Effects of Machining

General, localized, often hidden and sometimes unpredictable damage is imparted to the substrate periphery during typical machining operations. This has been a wide spread problem throughout the entire composites industry for decades . . . and the XYZ C-C/SiC machining approach offers no improvements in this area. As a matter of fact, due to the brittle nature of the constituents, CMC systems in general are more vulnerable to traditional machining methods than ordinary PMC structures. In more recent times, water-jet and laser machining techniques have greatly minimized this type of damage but not all composite structures can utilize these methods. Without a doubt however, composite billets and panels have to be cut to the desired shapes and dimensions, so there is no getting around the necessity and requirements for machining, but the damaging effects cannot simply be downplayed or ignored either.

Whether or not surface damage is imparted to the articles when they are machined is not the question because there is convincing evidence from past HT tests indicating the presence of this damage in failed articles. The main two issues are concerned with how extensive and penetrating the surface damage is and to what degree of restoration is achieved along the affected peripheral fiber-to-matrix interfaces by the subsequent PIP #11 process, if any at all. Specifically, the concerns would deal with the level and quality of repair imparted to the damaged interfaces in terms of chemical bond restoration and the re-establishment of mechanical interlocks between the matrix and the fiber along the outer fringes of the substrate. Mechanical interlocking is responsible for the exceptionally strong general adherence of Layer 1 to the substrate, but the nature of chemical binding and/or a possible phase transition zone between the 1550° a-SiC layer deposited during PIP cycle #11 and the 3000° β-SiC in the machined substrate is not well understood.

While the z fiber bundles offer continuous reinforcement properties across the entire length of the pintle article, the machining process vastly reduces the length of perpendicular u-v-w bundles

comprising the lateral reinforcement. Consequently, *u-v-w* bundles located closest to the pintle shaft circumference edges, as well as those local to the pintle head apex, become the shortest bundle segments within the entire body. The value of these shortened bundle segments (or bundle stubs) to the overall composite integrity is questionable. More importantly however, they are most vulnerable to extraneous forces, excessive localized porosity and excavation effects. It is certainly conceivable that some of these shortened, outer bundle segments would be susceptible to machining agitation and could possibly be loosened or dislodged during the machining process. Additionally, the presence of intersection voids and localized porosity surrounding some of these bundle segments reduces the fiber-to-matrix bonding contact area and increases the likelihood of extraction.

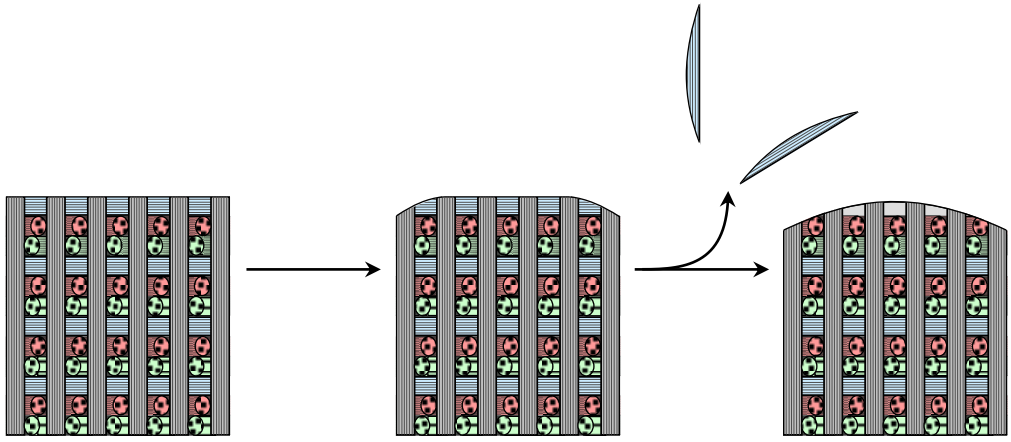

PIP cycles 11-13 leave a smooth, tightly adhered coating to the machined article surface but with minimal 'fill and fare' effects. Thus, a spallation event exposing Layer 1 might reveal these missing bundle segments as indentations or short trench-like depressions similar to those indicated in the photos. After all the outer PIP and Seal Coat layers have been applied and fired, these indentions are probably not even noticeable on the finished article. It is suspected that if Layers 4, 3 and 2 could be safely stripped from the surface, these kind of trench-like depressions could be seen periodically *all over* the surface of the articles. In other instances, some of the loosely bound bundle segments, which happen to stay on throughout the machining process, may ultimately dislodge and become liberated during an excavation/spallation event as the burn cycle takes place. These kind of impressions could contribute to the longitudinal trenches seen in the tire track pattern, where it almost appears as though the bundle segments were ripped out during the test process, perhaps late in the burn cycle or just as it ended.

While it is typical in most composite systems for the reinforcement to carry the majority of the applied loading forces in almost all directions, this is not necessarily the case in these particular (machined) CMC articles. Considering the facts that the fiber volume fraction in the C-C/SiC system is astonishing low, none of the fiber bundles are interlocked or woven together and, other than the *z*-direction, all of the fiber bundles are short, discontinuous segments, analogous to nothing more than an ordered array of isolated chopped fibers separated by relatively wide spaces with little-to-no intimate contact, laminar nesting or meshing interaction at all. The only stress direction in which the fibrous reinforcement genuinely dominates the action is along the *z*-axis under tension, which is due to the continuous nature of the reinforcement in this direction. Under compressional forces, the matrix is expected to carry the entire load *in all directions* and at all temperatures, regardless of the quantity or orientation of embedded fiber bundles (compared to the ceramic phase, carbonized PAN fiber compressional properties are minuscule and play no significant role in these types of loading). During the early stages of bending, the stiff matrix tries to dominate. But on the tension side, after

the matrix ruptures, fiber bending and tensional toughness factors begin to play an increasing role, while the matrix dominates on the compression side throughout. Ultimately, the z-axis fiber bundles assume a prominent role in the multi-modal flexural failure process, but due to the unusually low fiber volume fraction, their benefits are severely limited and, from a mechanical standpoint, this configuration is vastly inferior to more typical composite fiber volumes in the 55-70% range. As a result, all the mechanical properties ordinarily recognized and attributed to the fibrous reinforcement in most composite platforms do not really apply to this particular CMC system.

Molten Metal Splatter

During the HT-7 investigation, similar splotches of metal were seen on some of the valve component surfaces. Later on, EDX analysis indicated that these metal remnants were comprised of almost equal (atomic) proportions of silicon and calcium. Identification of the exact sources responsible for generating such external quantities of these elements in the valve environment was not conclusive. However, a probable scenario is available. Above about 2000°F, even in a mildly oxidative environment, a 5th layer will tend to form on the surfaces of the SiC components which is comprised of glassy (vitreous) silica, SiO_2. While this oxide layer is very thin and perhaps spotty across the surfaces, it is capable of reacting with other elements (or compounds) at high temperatures, even below its melting point. It will melt above 3000°-3100F° but will begin to undergo solid state sintering and interparticle surface diffusion as low as 2200°-2400°.

The use of calcium-based reducing agents and drying/dehydration compounds during the synthesis of SMP-10 polymer has already been substantiated (via exchanges with Starfire's founder and chief scientist). Remnants or residual traces of these calcium compounds are likely to be present in finished SMP-10-based products. It is suspected that during the burn cycle, these remnant compounds break down, releasing elemental calcium, which then migrates (or 'blooms') to the surface where it immediately reacts with available oxygen to form CaO. Subsequent reaction of CaO with surface SiO_2 gives the predominant mixed oxide calcium silica, $CaSiO_3$, which melts around 2800°-2900°. Thus, during the > 2200°-2600F° range of the burn cycle, surface oxidation of the outer SiC layers accelerates which reacts with blooming CaO to form $CaSiO_3$. However, exhaust gases from the motor burn are not necessarily those of an aggressive oxidation atmosphere since they consist heavily of the *products of oxidation* and are more representative of a *depleted* oxidation environment. At the tail end of the burn cycle, gases passing through the valve chamber create a *deoxidizing* atmosphere, which facilitates reduction of the $CaSiO_3$ oxide into the CaSi intermetallic. CaSi alloy exhibits a deep eutectic which melts around 2300°-2400°F, however, slightly oxidized CaSi alloy will have an even higher melting point. Alternative reaction paths might have the elemental calcium reacting directly with SiC or SiO_2 to form the intermetallic.

At the hottest peak of the burn cycle (after most of the spallation events have already occurred), it is surmised that molten agglomerates or globules of CaSi become highly mobile and possibly even 'air born' due to flow turbulence. Perhaps they are expelled out of the nozzle momentarily before the cycle shuts off. Remnant globules then rapidly deposit (or splatter) onto regional hot surfaces where they solidify. This is analogous to molten solder which is always attracted to and migrates toward the hottest surfaces. There is no solid evidence in support of this theory and there may be points that are not totally precise, but it does provide one possible explanation for the appearance of the metallic anomalies seen on these surfaces.

In various exchanges over the years with the chief developer of SMP-10 pre-ceramic polymer, the issue has specifically been raised concerning the nature and strength of interactions between the crystalline and glassy phases of ceramicized SMP-10 in terms of chemical bonding and mechanical interlocking within an envisioned a-SiC-to-β-SiC transition zone or interphase (if there is one). The exact mechanisms involved are not well understood, and there is no evidence that a unique conversion zone even exists. It is clear however, that the bonds which form between *β*-SiC and a-SiC phases cannot compare to the strong interactions joining crystalline *β*-SiC interfaces together which have been processed to 2600°F or higher. Most importantly, as a result of the property differences between these two polymorphs, a-SiC/*β*-SiC interfaces will undoubtedly be subjected to unexpected stresses during temperature excursions which could have questionable effects. An interesting issue for the present case might be one that concerns the nature and strength of bonding between interfacing glassy layers which have been thermally processed to varying degrees of green ceramic conversion early during the polymer-to-glassy-to-crystalline reaction/transition pathway.

While dendritic-type mechanical interlocking effects are known to occur within certain bimaterial systems, functional transition gradients and long range conversion zones are typically established by robust chemical diffusion processes between the phases. For C/C and ceramic systems, functional gradients are generally driven by high temperature reaction kinetics so that thermochemical diffusion of reactants generated from one phase infiltrate or diffuse into the micro/mesoporosity of the adjoining interface where they encounter reaction sites, ultimately forming a very strong dendritic bonding network comprised extensively of both strong chemical links and penetrating mechanical interlocks permanently joining the two phases. For constituents containing an appropriate balance of macro-, meso- and microporosity channels and a reaction affinity towards the other phase, both mechanical and chemical interlocking effects become highly prominent so that the two phases essentially become 'locked' together requiring the application of extreme mechanical forces to separate the two. This is analogous to the functional gradient transition zone established during the pack-cementation conversion process used on the Shuttle's Reinforced Carbon/Carbon (RCC) which essentially 'fuses' the SiC phase to porous C/C substrate. There are no indications that anything of this nature occurs here nor that any apparent chemical diffusion effects are established within the current C-C/SiC system between the carbonized pitch phase, the fibrous phase, or either of the SiC phases. Thus, it is believe that no (significant) transition zones are developed anywhere in the current FMI C-C/SiC system and that all constituents exist independently, essentially retaining discrete boundaries at all the interfaces. The implication then is that, under the right conditions, most of the interfaces within the C-C/SiC system are separatable under limited force applications.

However, significant mechanical interlocking effects are believed to exist within the XYZ C-C/SiC system, particularly along the substrate-to-Layer 1 interface, as well as fiber-to-*β*-SiC interfaces. Some of the chemical bonding mechanisms known to occur along C-C, C-SiC and SiC-SiC interfaces in the C-C/SiC system include free radical addition (via cross-linking with allene side groups), reduction to carbosilane (with and without the release of hydrogen), potential condensation reactions (possibly expelling small amounts of oxygen, water, silicon oxides and/or small aliphatics), and weak interactions between carbonaceous phases. Van der Waals attractions, pi orbital overlap, C-C sigma bonds, siloxane linkages, carbosilane bonds and possibly alkoxy links are also typical. All other traditional binding mechanism would not survive the thermal processes the material is subjected to during the manufacturing process and many of the aforementioned mechanisms would not survive either (they were listed as possibilities). Thus, the primary binding mechanism joining interfaces throughout the C-C/SiC system is essentially mechanical in nature.